ACS OMEGA

http://pubs.acs.org/journal/acsodf

Article

# Curing Time Impacts on the Mechanical and Petrophysical Properties of a Laponite-Based Oil Well Cement

Abdulmalek Ahmed, Ahmed Abdulhamid Mahmoud, and Salaheldin Elkatatny*

Cite This: *ACS Omega* 2022, 7, 31246−31259

Read Online

ACCESS | Metrics & More | Article Recommendations

**ABSTRACT:** Throughout the life of a well, the cement sheath is exposed to several loadings, which can harm its key properties and impede its functions. These loadings become more significant at the early age of forming the cement sheath in which the properties of the cement are not completely developed. In this study, 10 cement samples with and without laponite particles were prepared and cured for five different periods (6, 12, 24, 48, and 72 h). The failure properties, petrophysical parameters, elastic properties, and density variation along the samples were examined. All of the samples were characterized by nuclear magnetic resonance and X-ray diffraction to understand the influence of the curing times on the cement properties. The results showed that the compressive and tensile strengths of both cement systems increased with the curing time and the incorporation of the laponite particle increased the strength of the cement. The permeability of both cement samples decreased with curing time, and the addition of laponite also decreased the permeability of the cement samples because of the presence of laponite-clay particles. The addition of laponite particles also increased the elasticity of the cement as indicated by the decrease in Young's modulus and the increase in Poisson's ratio. Logarithmic relationships were established to represent the changes in porosity, compressive strength, and tensile strength, while the changes in the other properties of permeability, Poisson's ratio, Young's modulus, and density variation were represented accurately with power-law equations.

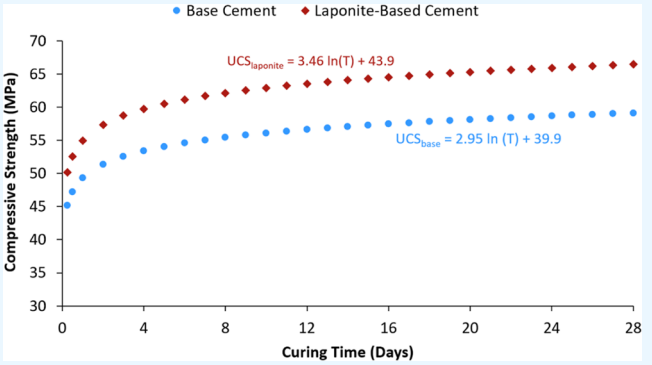


## 1. INTRODUCTION

In the petroleum industry, when the casing is run into the well to endure the forces of collapse and burst, a slurry of cement is pumped to fill the annulus between the steel casing and rock formation.[1] The slurry starts to harden gradually, and the cement sheath is formed. The cement sheath plays a vital role in the well integrity by providing zonal isolation and prevention of fluids movement between different formations, protecting the casing string against corrosion, and providing mechanical support to the casing and the drilled formations. The failure of cement sheath could lead to annulus pressurization, migration of formations fluid to the surface, and blowout in disastrous cases. The hazard of cement failure could be diminished by designing a high-quality cement sheath that warrants the essential integrity of the well, reduces the risk of failure coming from the accumulated materials produced by the physicochemical process, and stops the formation's fissures at the interface between cement and casing and between cement and rock.[2]

Recently, many researchers have focused on the addition of several materials to the cement slurry to improve its performance, increase the valuable life span of the well, and minimize costs resulting from the failures in the cement matrix. One of these additives is laponite which is a natural inorganic source containing mainly silicate. It is used as an additive to modify and enhance the rheological properties of many products.[3−5] Laponite has many advantages such as developing the viscosity of the formulation by reacting with the soluble components,[6] dispersing in water,[7,8] and preventing solid aggregation by enhancing its dispersibility.[9−13] A recent study conducted by Elkatatny[14] showed the capability of laponite to enhance the homogeneity of the cement paste and minimize the density distribution along the column of cement. Laponite also increased the gel strength property without any negative impact on the plastic viscosity. In aqueous situations, laponite degrades into bioactive products that influence cement hydration in various stages and lead to the acceleration of the cement regeneration process.[15] Results showed that unique characteristics of laponite such as aptitude of swelling, the capacity of cation exchange, the aptitude of gel formation, and

**Received:** June 4, 2022
**Accepted:** August 17, 2022
**Published:** August 23, 2022





https://doi.org/10.1021/acsomega.2c03491
*ACS Omega* 2022, 7, 31246−31259

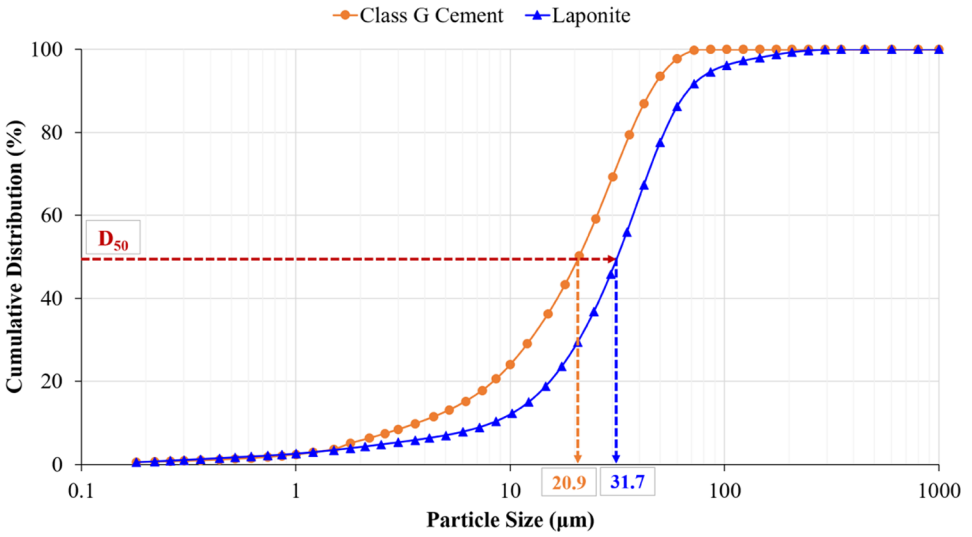


**Figure 1.** Particle size distribution of Saudi Class G cement and laponite.

the capacity of adsorptive are because of its high specific surface area, surface charge, and suitable interaction with inorganic and organic resources.[16]

The cement paste is a porous material that develops progressively by changing its state gradually from fluid to solid throughout the hydration process. During cementing process, various compositions of slurries can be utilized, and their hydration takes place at various conditions of pressure and temperature based on the depth. Subsequently, at a given period, cement paste properties rely upon the cement powder composition, water-to-cement (w/c) ratio, other additives, and hydration conditions regarding temperature, time, and pressure. Moreover, throughout the life of oil wells, the cement sheath is exposed to several mechanical and thermal loadings, which can harm the cement sheath properties and modify its exhibition. During oil well drilling, the pressure can reach more than 40 MPa, while during the casing test, the pressure is varying between 10 and 80 MPa depending on the type of reservoir.[17] These loadings can lead to cement sheath deformation and accordingly the formation of cracks in the interface of casing-cement or rock-cement. This is especially significant when these loadings are applied at a generally early age when the mechanical properties and strength of the cement are not yet totally created. However, the shrinkage of cement and the reduction of its pore pressure at the early stages are known to be the most reasons for leakage in wells.[18−20] Nevertheless, a few experimental studies on evaluating the hydrating of oil well cement in field conditions and at different curing times were performed. Most of these studies were concentrated only on the mechanical properties such as compressive and tensile strengths or the elastic properties such as Poisson's ratio and Young modulus.[21,22] However, previous studies did not evaluate the effects on the petrophysical characteristics such as porosity and permeability and did not evaluate the change in the mechanical and petrophysical properties with the development of the hydration process at the early age of hydration. This information is important especially for new cementing systems such as the cement slurry incorporating laponite particles which is considered in this work.

There are several experimental methods to examine the early age properties of the cement sheath. Some ways focus on the rate of reaction, while others investigate the chemical or physical properties of the cement at different time intervals.[23,24]

This paper is dedicated to evaluating the changes in the cement matrix properties at the early stages of the hydration process for the cement prepared with and without laponite particles. Several properties such as compressive strength, tensile strength, porosity, permeability, Poisson's ratio, Young modulus, and density variation (DV) were evaluated during the first 3 days of curing. All of the cement samples were characterized by several techniques such as nuclear magnetic resonance (NMR) and X-ray diffraction (XRD) to understand the influence of the curing times on the cement properties. The different properties are evaluated at different curing times of 6, 12, 24, 48, and 72 h.

## 2. EXPERIMENTAL PROGRAM

**2.1. Materials and Techniques.** The primary materials used in this study are class G cement and laponite. Class G cement is generally mixed with several additives such as silica flour, retarder, accelerator, deformer, extender, dispersants, fluid loss agents, and weighting materials to enable covering a wide range of wellbore conditions.

Class G cement used in this study was provided by a service company. The chemical composition of the cement was attained via X-ray diffraction (XRD). After performing the XRD measurement, the raw data were processed and quantified using the Rietveld method and HighScore Plus software. The XRD result indicates that class G cement considered for this study composed of tricalcium aluminate ($C_3A$) <1%, tricalcium silicate ($C_3S$) = 65%, dicalcium silicate ($C_2S$) = 15%, and tetra calcium aluminoferrite plus twice tricalcium aluminate ($C_4AF + 2\ C_3A$) = 18%.

The laponite used in this work is a synthetically modified phyllosilicate that has a 330 $m^2/g$ surface area and a 1000 $kg/m^3$ density. Due to its high specific surface area, laponite could accelerate the hydration kinetics of the cement slurry by stimulating the precipitation and nucleation process of calcium silicate hydrate (C−S−H) as a mass during the early time of reaction.[25,26] This phenomenon causes matrix densification through the quick filling of the space between the grains of the



https://doi.org/10.1021/acsomega.2c03491
ACS Omega 2022, 7, 31246−31259

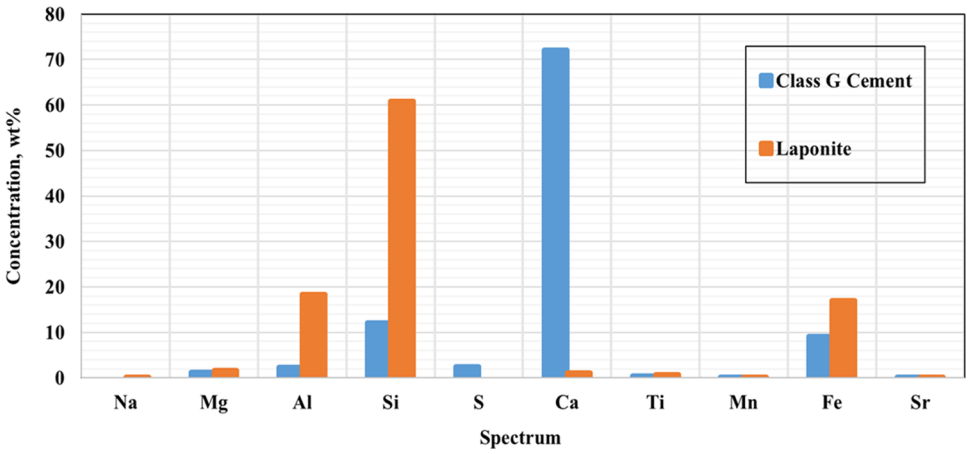


**Figure 2.** Compositions of class G cement and laponite used in this study, by XRF analysis.

cement with hydrated phases; so, increasing the compressive strength and decreasing the cement matrix porosity.[27−29]

The particle size distribution for both class G cement powder and laponite was obtained via the wet dispersion unit ANALYSETTE 22 Nano Tec plus instrument. The results reveal that the median size of the cement is 20.9 $\mu$m which is 34.1% smaller than the median size of laponite that is 31.7 $\mu$m, as shown in Figure 1.

The elemental compositions obtained via X-ray fluorescence (XRF) were performed using M4 TORNADO, which uses small-spot micro X-ray fluorescence. Powder samples were used in the measurement to detect the elements, and MicroXRF (Bruker) configured with a micro-focused rhodium source (50 kV, 600 $\mu$A) and a polycapillary optic (~20 $\mu$m spot size) was used to acquire the elemental spectra of the samples. Proprietary M4 software package was used to quantify elemental intensities from the spectra data.

The results of XRF illustrate that laponite has 60% silicon compared to only 12% present in class G cement, whereas the cement has a high amount of calcium (72%) compared to only 1.2% in laponite as depicted in Figure 2. It is also presented that laponite has a high amount of aluminum ($Al^{3+}$) and iron ($Fe^{2+}$) which are 18 and 17%, respectively. These elements in laponite will lead to a kind of pozzolanic reaction with the high amount of Ca presented in cement. Throughout the hydration dynamic, the reaction between silicon and calcium ions results in the formation of calcium silicate hydrates (CSH), where this CSH could increase the compressive strength.[30,31] Here, the $Al^{3+}$ freely goes into the calcium silicate hydrate of the cement, where this replacement has a significant influence on different characteristics of the chemical performance of the cement.[32−36]

**2.2. Slurries Preparation.** The cement slurries were prepared based on the API standards API[37] and API.[38] The base cement was prepared to contain class G cement, 0.7% by weight of cement (BWOC) of the fluid loss additive, 35% BWOC of silica flour, 0.1% BWOC expandable material, 0.08% BWOC of dispersant, 2.82 × $10^{-6}$% BWOC defoamer, and 44% BWOC water. In addition to the additives considered to make the base slurry, 0.3% BWOC of laponite was added to another new slurry to make the laponite-based cement slurry; this concentration of laponite was considered according to the recommendation of Elkatatny.[14]

**2.3. Experimental Techniques.** After the preparation, all of the slurries were poured inside cubical and cylindrical molds based on the needed tests. Then, the molds were placed inside a water bath full of distilled water at a temperature of 170 °F, the samples were allowed to cure for different durations of 6, 12, 24, 48, and 72 h. After each period of curing time, samples representing the base and laponite-based cement were removed from the molds and subjected to several tests such as failure tests, petrophysical tests, elasticity tests, density variation, nuclear magnetic resonance (NMR), and X-ray diffraction (XRD).

*2.3.1. Failure Tests.* Two failure parameters of the compressive and tensile strengths were evaluated for all samples after the different curing periods to study the effect of curing time on the strength of the laponite-based cement samples. Cubical cement samples with edges of 2.0 in. were used for the compressive strength test as recommended by the standard ASTM.[39] For the tensile strength, the Brazilian test was conducted to measure the indirect tensile strength using a cylindrical sample of 1.5 in. diameter and 0.75 in. thickness followed the ASTM[40] standard. During the tests, the samples were loaded at a constant rate of 1.5 kN/s. The compressive and tensile strengths of every cement sample at the specific curing time were evaluated on three different specimens and the average strength of the three measurements was considered as the compressive or tensile strength for that sample.

*2.3.2. Petrophysical Tests.* The petrophysical properties of the porosity and permeability were evaluated for all samples considered in this study at the different curing periods to investigate the influence of the curing time on the petrophysical properties of the laponite-based cement samples. Samples of 1.5 in. diameter and 1.0 in. thickness were used for petrophysical properties evaluation. The permeability and porosity were measured by the automated porosimeter−permeameter based on the length and diameter of samples, gas viscosity, gas flow rate, and pressure drop.[41] The measurements were conducted using nitrogen under an applied pressure of 1200 psi, confining pressure of 500 psi, and room temperature.

*2.3.3. Nuclear Magnetic Resonance (NMR).* NMR was applied to evaluate the effect of curing time on the pore size distribution and porosity changes for the laponite-based cement samples. Measurements of the relaxation time ($T_2$) were performed on cylindrical cement samples with a diameter of 1.5 in. and length of 4.0 in. utilizing NMR with a low magnetic field to cause nuclear spin-precession that is easily detected. A 2 MHz of magnetic field was used by the NMR


https://doi.org/10.1021/acsomega.2c03491
ACS Omega 2022, 7, 31246−31259

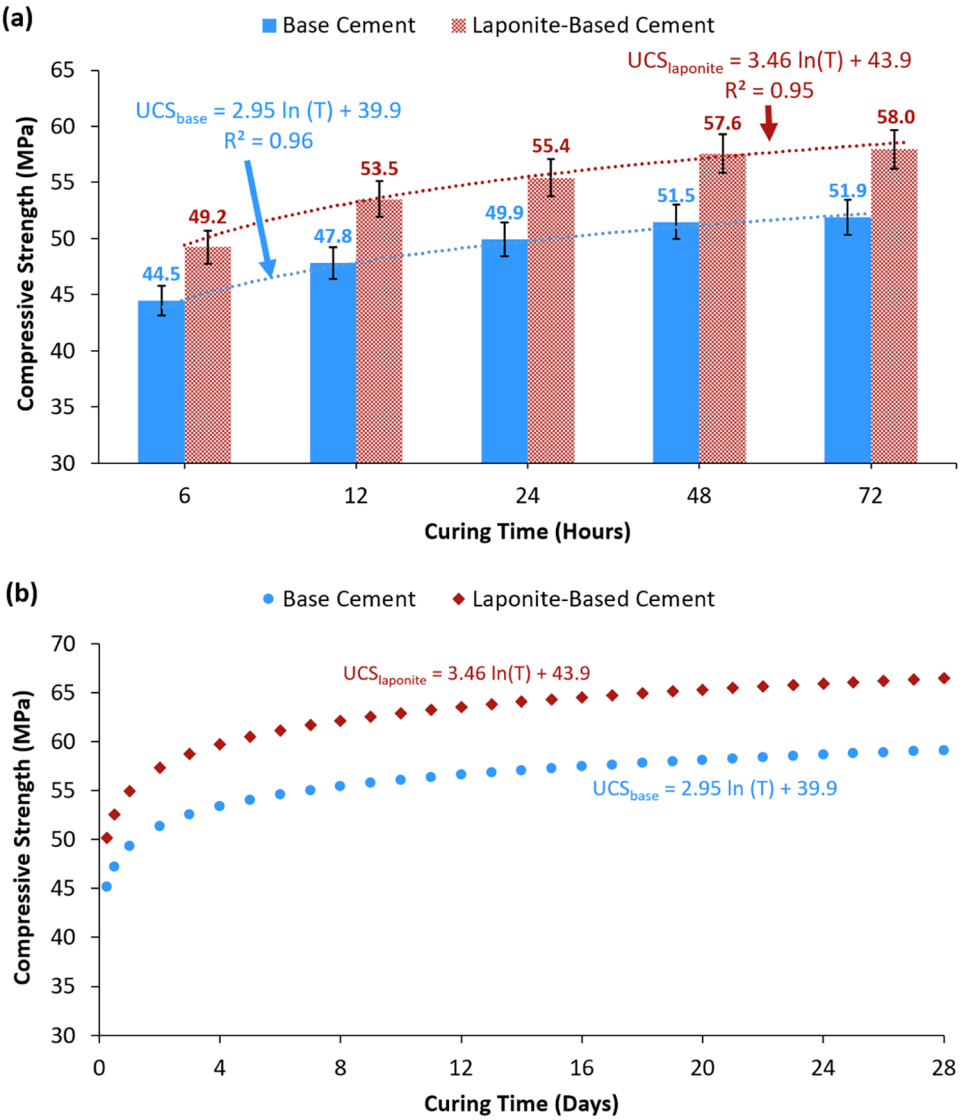


**Figure 3.** Compressive strength at different curing times for the two cement systems. (a) Results of the compressive strengths for the two cement systems at curing times of 6, 12, 24, 48, and 72 h. (b) Expected changes in the compressive strength of both cement systems for 28 days.

spectroscopy system "Geospec rock analyzer" from Oxford Instruments.

*2.3.4. Elasticity Test.* Young modulus and Poisson's ratio were measured to examine the impact of the curing time on the elastic properties of the laponite-based cement samples. Cylindrical samples with a length of 4.0 in. and a diameter of 1.5 in. were used to evaluate the cement elastic properties using the sonic mode of the scratch test machine. Then, the Young modulus and Poisson's ratio were obtained by measuring the ultrasonic velocities (i.e., pressure and shear waves).[42]

*2.3.5. Density Variation (DV).* Cylindrical samples having a diameter of 1.5 in. and a length of 4.0 in. were cut into three parts (bottom, middle, and top). The density of each part was determined by measuring its weight, area, and length. Then, the density variation across the cement samples was evaluated by taking the ratio of the difference between the top and bottom densities to the bottom density.

*2.3.6. Mineralogical Composition Analysis.* X-ray diffraction (XRD) was utilized to analyze the influence of the curing time on the changes in the hydration products of the laponite-based cement samples. Where the changes in the cement hydration over early periods (first 3 days of hydration) were investigated by XRD.

For XRD analysis, the spectra were acquired on a Malvern PANalytical EMPYREAN Diffractometer system at $2\theta$ range from 4 to 70° and 0.01° step size. The equipment used for XRD measurement was equipped with a Pixcel1D detector, a reflection-transmission spinner (minimum step size $\phi$: 0.1) sample stage, a Cu generator with K-$\alpha$1 [Å] = 1.54060, K-$\alpha$2 [Å] = 1.54443 and operated at a current of 40 mA and 45 kV.

## 3. RESULTS AND DISCUSSION

**3.1. Influence on the Failure Parameters.** Figure 3a summarizes the results of the changes in the compressive strengths of the base and laponite-based cement systems evaluated at different periods of curing time (72 h). Visibly, the increase in the curing time strengthened the early compressive strength for both cement systems. As indicated in Figure 3a, the laponite-based samples have higher compressive strength at all curing times.



https://doi.org/10.1021/acsomega.2c03491
ACS Omega 2022, 7, 31246−31259

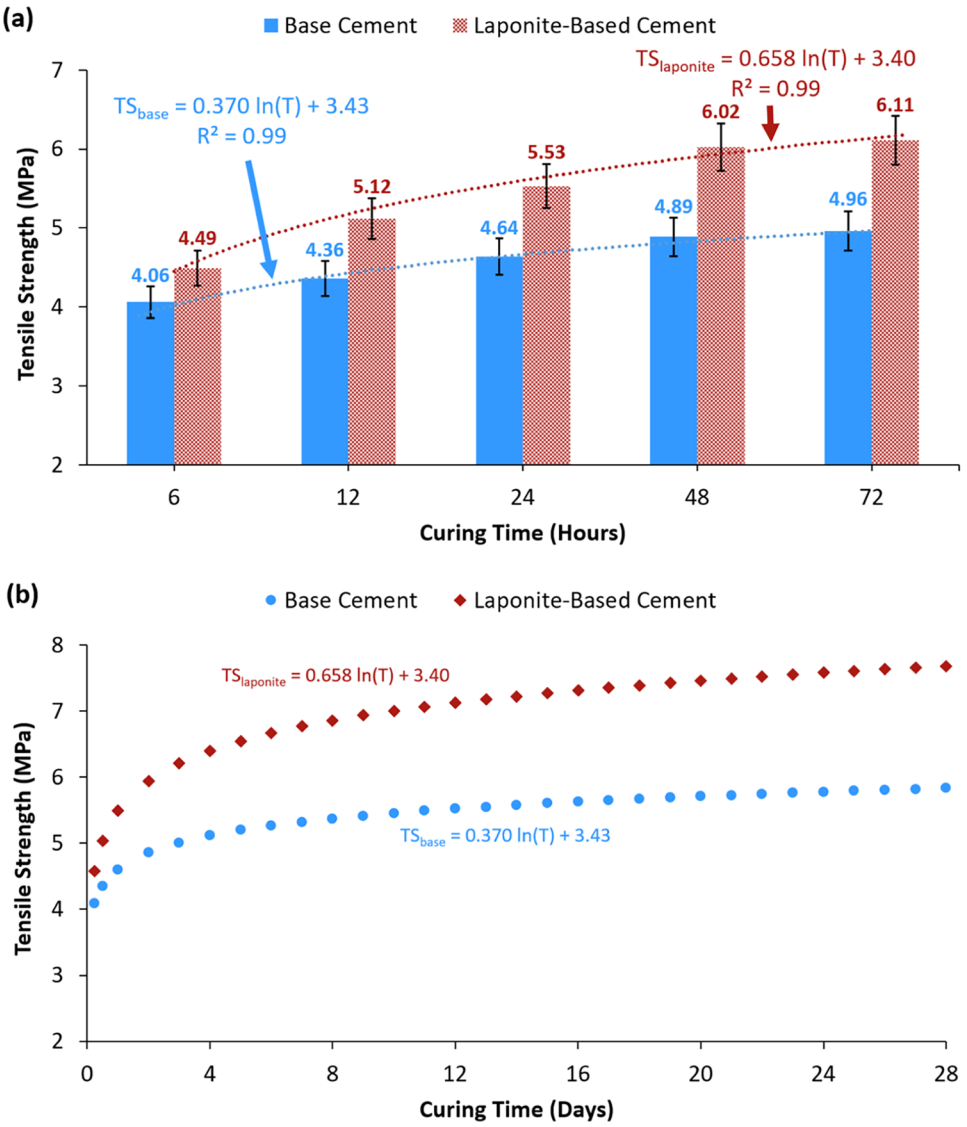


**Figure 4.** Tensile strength at different curing times for the two cement systems. (a) Results of the tensile strengths for the two cement systems at curing times of 6, 12, 24, 48, and 72 h. (b) Expected changes in the tensile strength of both cement systems for 28 days.

As indicated in Figure 3a, after 6 h of hydration, the compressive strength for the base and laponite-based samples are 44.5 and 49.2 MPa, respectively. The compressive strength for the base cement then increased slightly with time to stabilize after 48 h at about 51.5 MPa. For the laponite-based samples, the compressive strength increased and stabilized after 48 h of hydration also reaching 57.6 MPa. Both cement samples did not experience a significant increase in compressive strength after 2 days of hydration.

The changes in compressive strength of both systems with time were investigated mathematically to define the best relationship that descript these changes. This investigation indicated that the changes in the compressive strength for both base and laponite-based cement are best described by the logarithmic relationships of eqs 1 and 2 with correlation coefficients ($R^2$) of 0.96 and 0.95, respectively, as shown in Figure 3a.

$$UCS_{base} = 2.95 \ln(T) + 39.9 \quad (1)$$

$$UCS_{laponite} = 3.46 \ln(T) + 43.9 \quad (2)$$

where UCS is the unconfined compressive strength (MPa); $T$ is the curing time (h); and the subscripts base and laponite denote the base and laponite-based cement systems, respectively.

By applying eqs 1 and 2, the expected changes in the compressive strength of both systems under study were evaluated for 28 days as shown in Figure 3b. This figure shows that most of the changes in the compressive strength of both cement systems were during the first week of curing. After the first week, the changes in the compressive strength might be very small, and after 21 days of curing, the compressive strength of both systems could stabilize.

For the results of tensile strengths illustrated in Figure 4a, it is clear that the changes in the tensile strength agree with the changes in compressive strength for both systems. Wherein, the tensile strength increases with the increase of the early curing time and it is greater for the laponite-based samples at all curing times. The tensile strength was developed gradually in the base cement system, whereas in the laponite cement system, there was a sharp increase in the tensile strength during



https://doi.org/10.1021/acsomega.2c03491
ACS Omega 2022, 7, 31246−31259

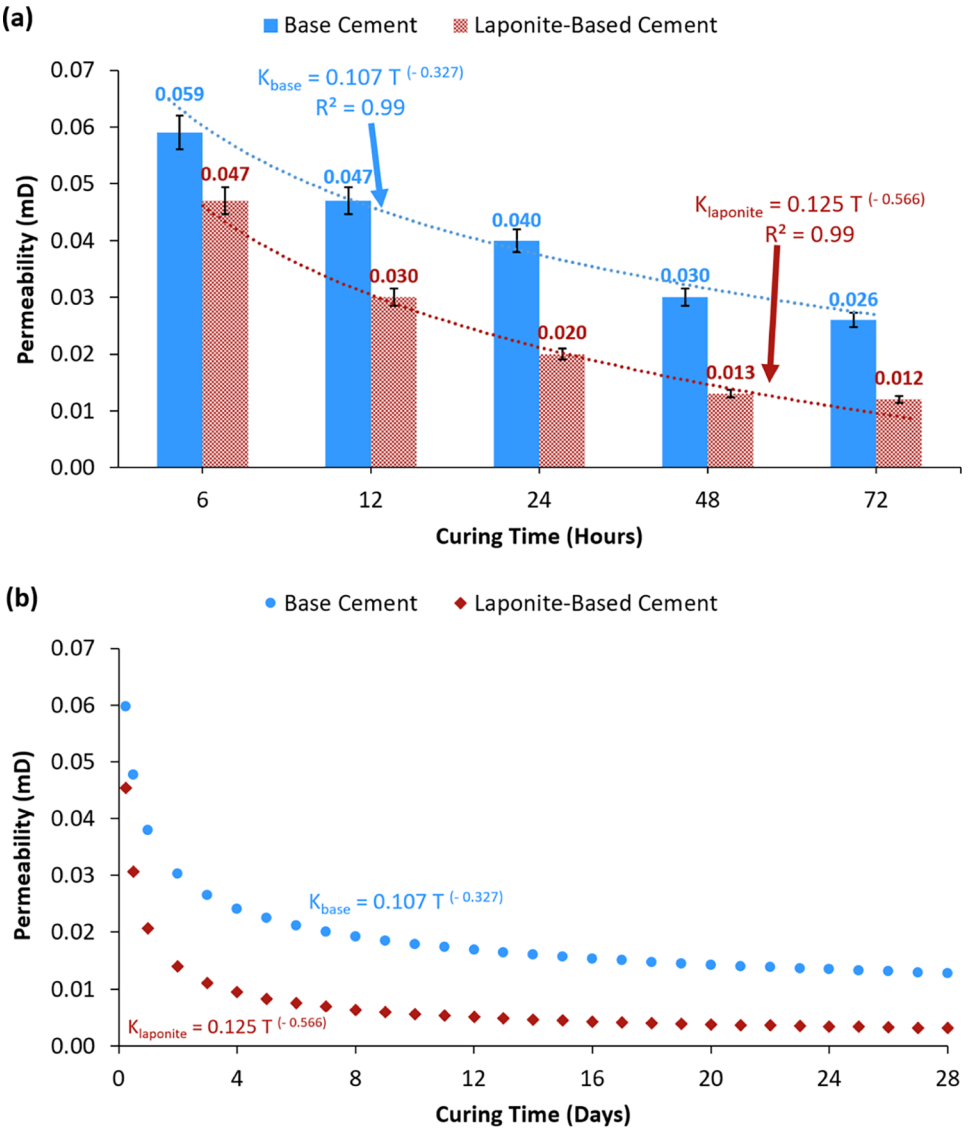


**Figure 5.** Permeability at different curing times for the two cement systems. (a) Results of the permeability for the two cement systems at curing times of 6, 12, 24, 48, and 72 h. (b) Expected changes in the permeability of both cement systems for 28 days.

the first 12 h of curing; then, the development in the tensile strength was gradual in the next 2 days.

After 6 h of hydration, the base and laponite-based samples have tensile strengths of 4.06 and 4.49 MPa, respectively. The tensile strength of both systems increased to reach 4.36 MPa for the base sample and 5.12 MPa for the laponite-based sample after 12 h of hydration. After the first 12 h of hydration, the tensile strength of both systems increased gradually until the end of the 48 h to reach 4.89 MPa for the base sample and 6.02 MPa for the laponite-based sample. The tensile strength of the base and laponite-based samples after 72 h of hydration were 4.96 and 6.11 MPa, respectively.

The regression analysis indicated that the change in the tensile strength of the base and laponite-based samples could be represented accurately ($R^2$ = 0.99) with logarithmic relationships of eqs 3 and 4, respectively, as shown in Figure 4a.

$$TS_{base} = 0.370 \ln(T) + 3.43 \quad (3)$$

$$TS_{laponite} = 0.658 \ln(T) + 3.40 \quad (4)$$

where TS is the tensile strength (MPa); $T$ is the curing time (h); and the subscripts base and laponite denote the base and laponite-based cement systems, respectively.

Equations 3 and 4 were then used to plot the expected changes in the tensile strength for both base and laponite-based systems during the first 28 days of hydration as shown in the plots in Figure 4b. As indicated in this figure, during the first 7 days of hydration, most of the development of the tensile strength of both samples is expected to take place, and there might only be a slight increase in the tensile strength, which almost tends to stabilize after 21 days for the base sample and after 24 days for the laponite-based samples.

**3.2. Influence on the Petrophysical Properties.** The permeability was measured for all of the cement samples at the five early curing times, the results are compared in Figure 5. These results show that after 6 h of curing the permeability of the base cement system was 0.059 mD, which then decreased gradually with the curing time, this rate of reduction in permeability was decreasing with time and the base sample reached 0.026 mD after 3 days of curing. The same trend was noted for the laponite-based sample, which had a permeability



https://doi.org/10.1021/acsomega.2c03491
ACS Omega 2022, 7, 31246−31259

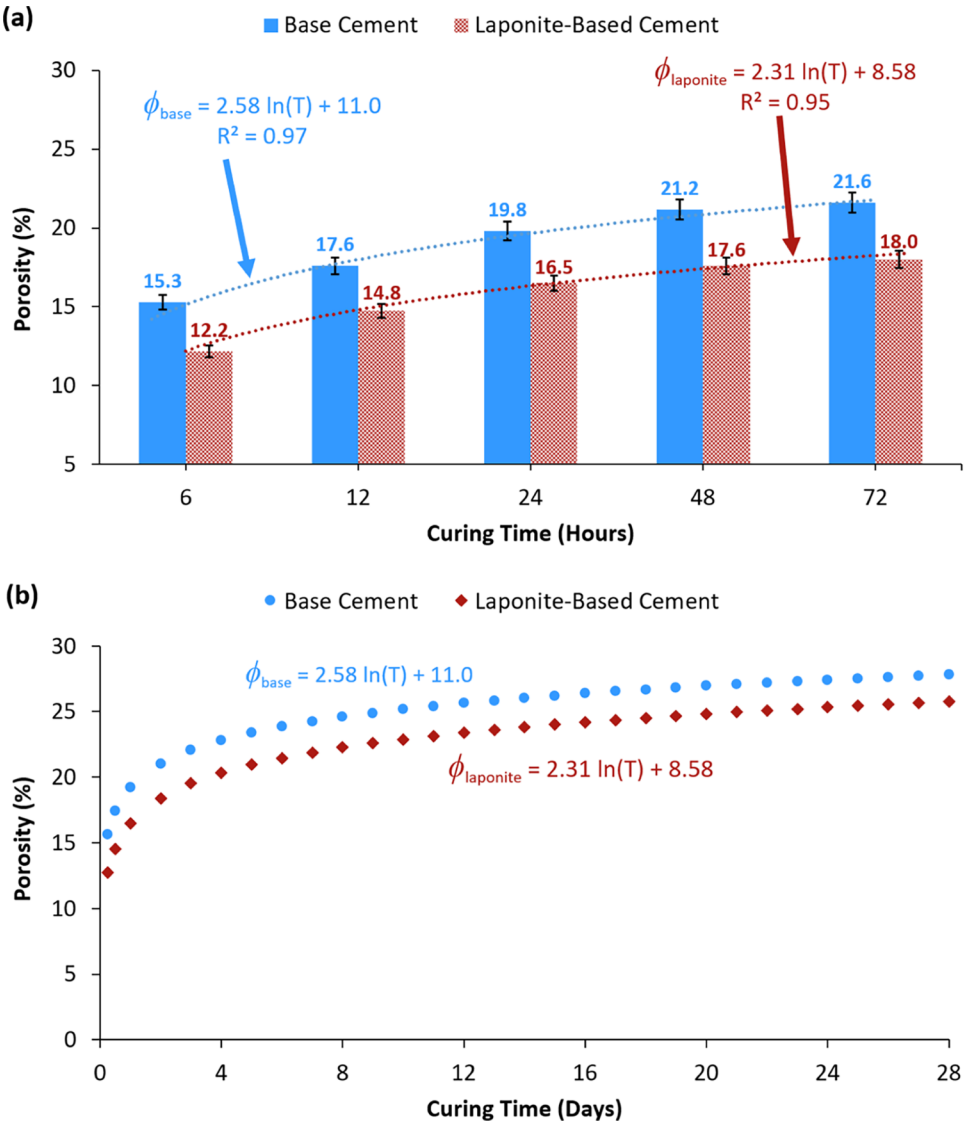


**Figure 6.** Porosity at different curing times for the two cement systems. (a) Results of the porosity for the two cement systems at curing times of 6, 12, 24, 48, and 72 h. (b) Expected changes in the porosity of both cement systems for 28 days.

of 0.047 mD after 6 h of hydration, and it was decreasing with the curing time with a high rate during the first 24 h of curing, then it tends to stabilize at the end of curing at 0.012 mD.

The changes in the permeability of the base and laponite-based systems with the curing time were also investigated mathematically to identify the best relationship to represent these changes. The results showed that the changes in the permeability for the base and laponite-based samples are best described by the power relationships of eqs 5 and 6 with a correlation coefficient ($R^2$) of 0.99 for both cement systems, as shown in Figure 5a.

$$K_{base} = 0.107T^{-0.327} \quad (5)$$

$$K_{laponite} = 0.125T^{-0.566} \quad (6)$$

where $K$ is the permeability (mD); $T$ is the curing time (h); and the subscripts base and laponite denote the base and laponite-based cement systems, respectively.

The expected changes in the permeability of the base and laponite-based samples for the first 28 days of hydration were then identified using eqs 5 and 6, respectively, as shown in Figure 5b. This figure shows that the permeability of both cement systems is expected to experience a considerable decrease within the first 7 days. The permeability will decrease until the end of week three but with a small rate compared to that of the first week of curing. After 24 days of curing, the permeability of both samples might stabilize.

Figure 6a summarizes the porosity change for the cement samples of the two cement systems after 6, 12, 24, 48, and 72 h of curing. Furthermore, it was observed that the porosity of both the base and laponite-based systems increased with the curing time. For the base samples, the porosity after 6 h was 15.3% which increased considerably to stabilize after 72 h of hydration at 21.6%. The porosity of the laponite-based samples after 6 h of hydration was 12.2%, which later stabilized after 72 h of curing at a value of 18.0%.

The regression analysis indicated that the change in the porosity of the base and laponite-based samples could be represented accurately with the logarithmic relationships of eqs 7 and 8 with $R^2$'s of 0.97 and 0.95, respectively, as shown in Figure 6a.



https://doi.org/10.1021/acsomega.2c03491
ACS Omega 2022, 7, 31246−31259

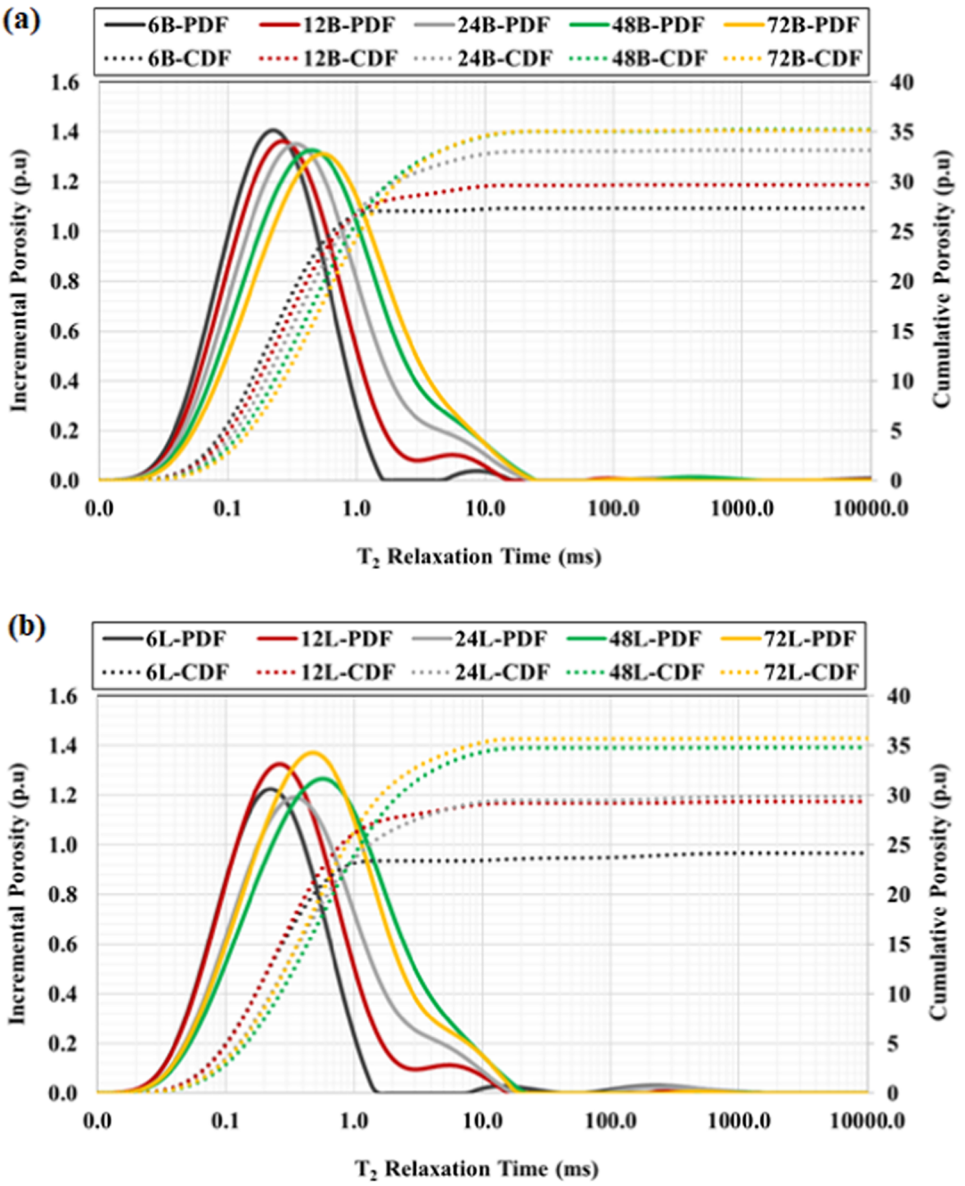


**Figure 7.** NMR $T_2$ relaxation for (a) base cement system and (b) laponite-based cement system, after 6, 12, 24, 48, and 72 h of curing.

$$\phi_{\text{base}} = 2.58 \ln(T) + 11.0 \quad (7)$$

$$\phi_{\text{laponite}} = 2.31 \ln(T) + 8.58 \quad (8)$$

where $\phi$ denotes the porosity (%); $T$ is the curing time (h); and the subscripts base and laponite represent the base and laponite-based cement systems, respectively.

Equations 7 and 8 were then used to plot the expected changes in the porosity for both base and laponite-based systems during the first 28 days of hydration as shown in the plots in Figure 6b. As indicated in this figure, during the first 7 days of hydration a significant increase in porosity with the increase of curing time for both cement systems is expected. This rate of increase will slow down, and the porosity might stabilize after 24 days of hydration, which is in agreement with the changes in permeability discussed earlier.

**3.3. NMR Characterization.** NMR was implemented to scrutinize the impact of the curing time on the pore size distribution of the two cement systems. Moreover, the pore distribution function (PDF) and cumulative distribution function (CDF) for the whole length of cement samples (4 in.) are plotted in Figure 7a for the base cement system and in Figure 7b for the laponite cement system. The results showed that for both systems as the curing time increases the porosity of the samples increased. For instance, in the base cement system (12, 24, 48, and 72 h of curing the porosities were 27.4, 29.7, 33.1, 35.2, and 35.3%, respectively). The same trend was observed in the laponite-based cement system (ich the porosities of the five curing samples 6, 12, 24, 48, and 72 h were 24.1, 29.3, 29.8, 34.8, and 35.7%, respectively). It can be seen that the porosity of NMR has a similar trend to the porosity obtained from direct measurement in Figure 6, in which the porosity increases with curing time even though the NMR porosity values are different from the porosity obtained from direct measurement; this is attributed to the difference in the measurement techniques.

**3.4. Influence on Elastic Properties.** Young's modulus and Poisson's ratio are considered the most important elastic properties of solid materials. Lower Young's modulus means high stability of the cement under shear stresses and higher



https://doi.org/10.1021/acsomega.2c03491
ACS Omega 2022, 7, 31246−31259

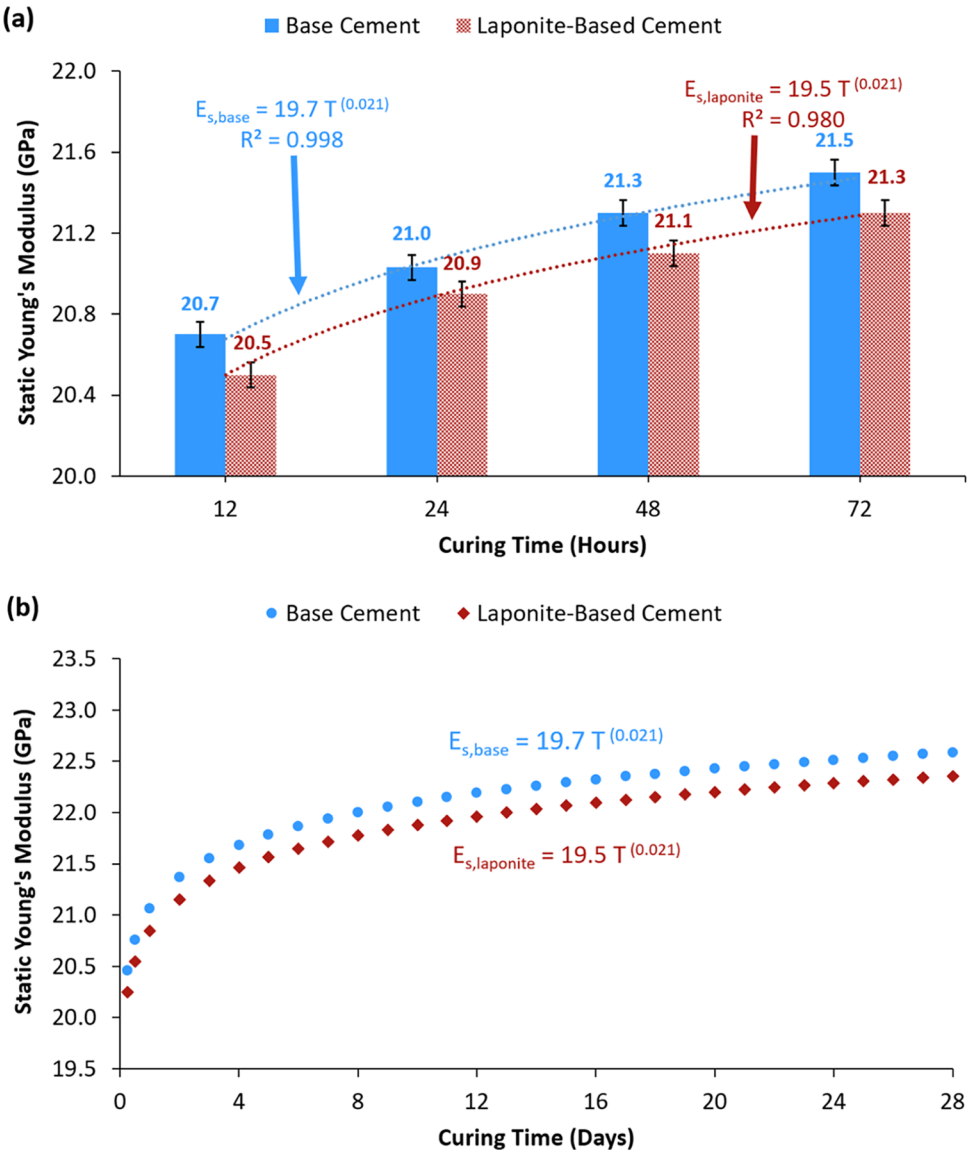


**Figure 8.** Young's modulus at different curing times for the two cement systems. (a) Results of the Young's modulus for the two cement systems at curing times of 12, 24, 48, and 72 h. (b) Expected changes in the Young's modulus of both cement systems for 28 days.

Poisson's ratio means low lateral expandability of the cement (Fjaer et al., 2007).[43] The effect of the curing times on Young's modulus of the base and laponite-based cement systems is illustrated in Figure 8a. As indicated in this figure, Young's modulus of the base cement after 12 h of curing was 20.7 GPa, wherein the value increased steadily until the end of the first 3 days of curing to reach 21.5 GPa at 72 h of curing. The same behavior was noted in the laponite-based cement for which Young's modulus after 12 h of curing was 20.5 GPa; then, it increased steeply with curing time to reach 21.3 GPa after 72 h of curing.

Moreover, it can be seen that, based on the results of Young's modulus, that laponite-based cement has a lower Young's modulus compared to the base cement, which indicates that the laponite-based samples are elastic and apply the same stress on both base and laponite-based samples will result in having a higher elastic strain on the laponite-based samples.

The changes in Young's modulus of the base and laponite-based systems with the curing time were also investigated mathematically to identify the best relationship to represent these changes. The results showed that the changes in Young's modulus for the base and laponite-based samples are best described by the power relationships of eqs 9 and 10 with $R^2$'s of 0.998 and 0.980, respectively, for both cement systems, as shown in Figure 8a.

$$E_{s,base} = 19.7T^{0.021} \quad (9)$$

$$E_{s,laponite} = 19.5T^{0.021} \quad (10)$$

where $E_s$ is the static Young's modulus (GPa); $T$ is the curing time (h); and the subscripts base and laponite denote the base and laponite-based cement systems, respectively.

The expected changes in Young's modulus of the base and laponite-based samples for the first 28 days of hydration were then predicted using eqs 9 and 10, respectively, as shown in Figure 8b. This figure shows that Young's moduli of both cement systems are expected to experience a considerable increase within the first 7 days. Young's modulus could increase until the end of 24 days but with a small rate


https://doi.org/10.1021/acsomega.2c03491
ACS Omega 2022, 7, 31246−31259

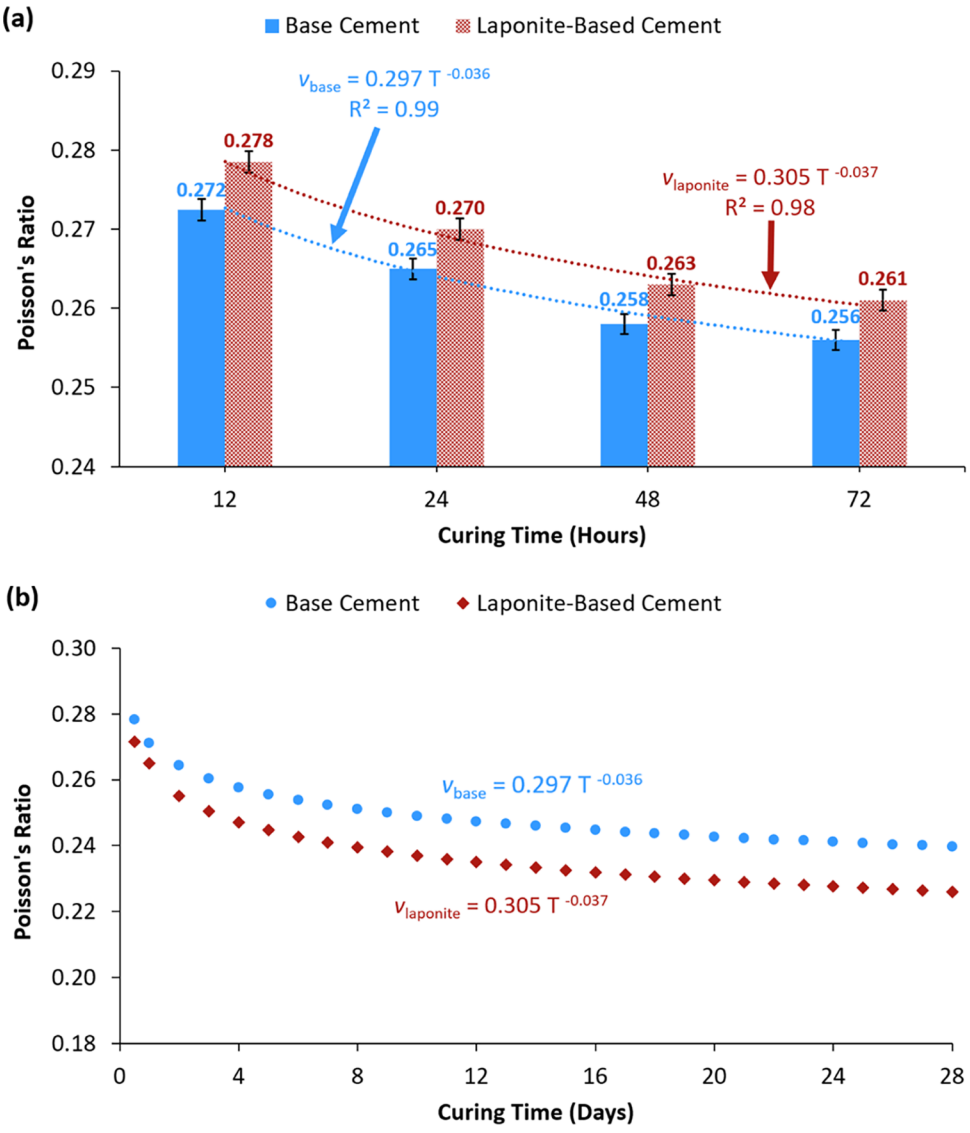


**Figure 9.** Poisson's ratio at different curing times for the two cement systems. (a) Results of the Poisson's ratio for the two cement systems at curing times of 12, 24, 48, and 72 h. (b) Expected changes in the Poisson's ratio of both cement systems for 28 days.

compared to that of the first week of curing. After 24 days of curing, Young's modulus of both samples will tend to stabilize.

For Poisson's ratio as shown in Figure 9a, after 12 h of curing it reached 0.272 for the base cement and 0.278 for the laponite-based cement. Poisson's ratio for both cement systems experienced a continuous decrease with curing to reach 0.256 and 0.261 for the base and laponite-based systems, respectively. The results in Figure 9 for Poisson's ratio showed that the laponite-based samples have a higher Poisson's ratio compared to those of the base samples at all curing times, which indicated high elasticity and low lateral expandability for these samples. This result agrees with the results of Young's modulus changes explained in Figure 8a.

The changes in Poisson's ratio for the base and laponite-based systems with the curing time were also investigated through regression analysis to find the best relationship to represent these changes. The results showed that the changes in Poisson's ratio for the base and laponite-based samples are best described by the power relationships of eqs 11 and 12 with $R^2$'s of 0.99 and 0.98, respectively, as shown in Figure 9a.

$$\upsilon_{base} = 0.297T^{-0.036} \quad (11)$$

$$\upsilon_{laponite} = 0.305T^{-0.037} \quad (12)$$

where $\upsilon$ represents Poisson's ratio; $T$ is the curing time (h); and the subscripts base and laponite are the base and laponite-based cement systems, respectively.

The changes in the Poisson's ratio for the base and laponite-based samples during the first 28 days of hydration were predicted using eqs 11 and 12, respectively, as shown in Figure 9b. This figure shows that Poisson's ratio of both cement systems will experience a considerable decrease between 12 h and 7 days of curing. Poisson's ratio will continue to decrease until the mid of the fourth week but with a small rate compared to that of the first week of curing. After 24 days of curing Poisson's ratio of both samples might stabilize.

**3.5. Influence on the Density Variation.** In many situations, the density distribution along the length of the cement column is not uniform due to the settling of the solid particles at the bottom of the cement column. Therefore, it is also important to investigate the impact of curing times on the



https://doi.org/10.1021/acsomega.2c03491
ACS Omega 2022, 7, 31246−31259

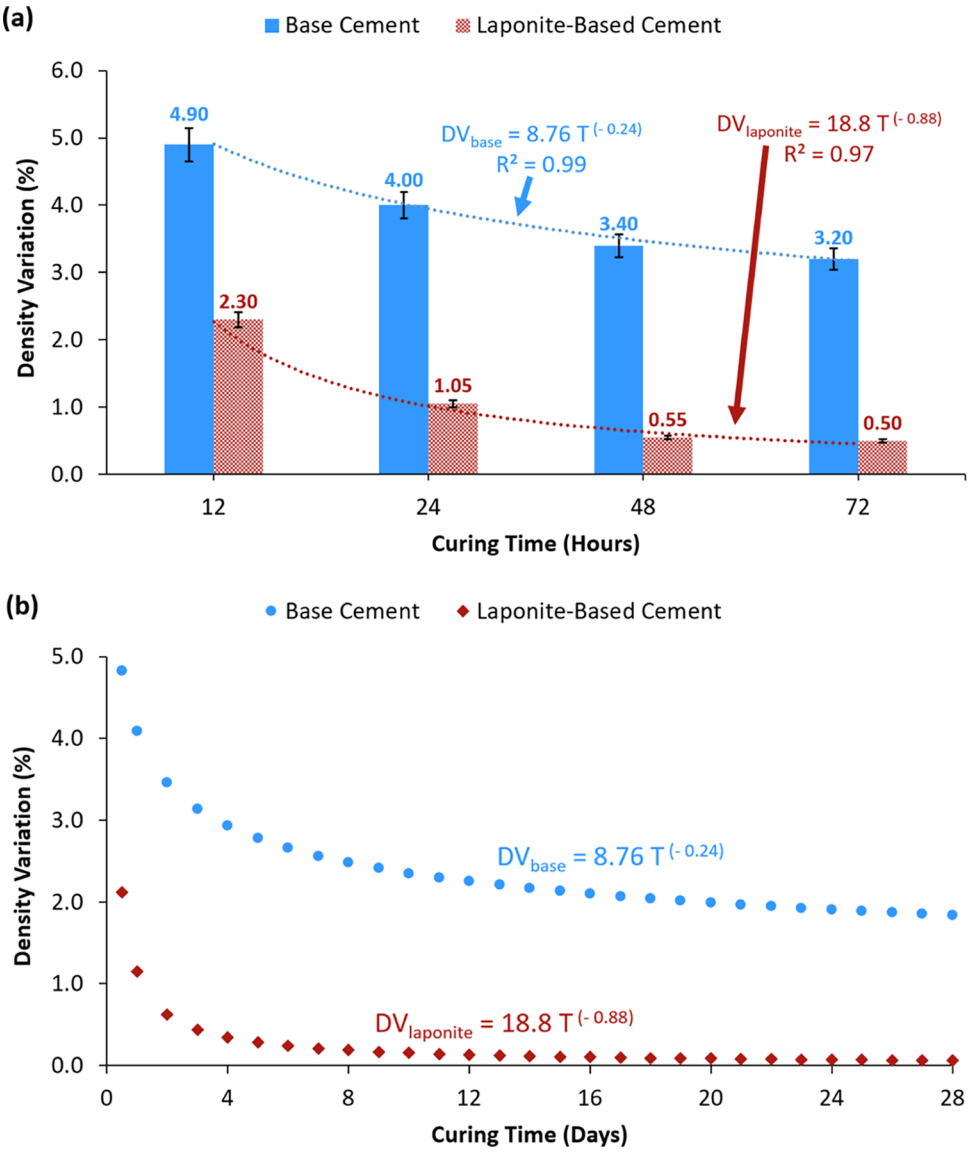


**Figure 10.** Density variation at different curing times for the two cement systems. (a) Results of the density variation for the two cement systems at curing times of 12, 24, 48, and 72 h. (b) Expected changes in the density variation of both cement systems for 28 days.

density variation along with the two cement systems under study (density variation between the top and bottom of the samples) as a function of curing time.

As shown in Figure 10a, after 12 h of curing, the density variation for the base and laponite-based samples are 4.9 and 2.3%, respectively. Density variation was then decreased until 72 h of curing to reach 3.2% for the base sample and 0.5% for the laponite-based sample.

The regression analysis indicated that the change in the density variation of the base and laponite-based samples could be represented accurately with the power relationships of eqs 13 and 14 with $R^2$'s of 0.99 and 0.97, respectively, as shown in Figure 10a.

$$DV_{base} = 8.76T^{-0.24} \quad (13)$$

$$DV_{laponite} = 18.8T^{-0.88} \quad (14)$$

where DV denotes the density variation (%); $T$ is the curing time (h); and the subscripts base and laponite represent the base and laponite-based cement systems, respectively.

Equations 13 and 14 were then used to plot the expected changes in the density variation for both base and laponite-based systems during the first 28 days of hydration, as shown in the plots in Figure 10b. As indicated in this figure, during the first 7 days of hydration, a significant decrease in density variation with the increase of curing time for both cement systems is expected. This rate of decrease will then slow down, and the density variation along the samples might tend to stabilize after 24 days of hydration.

**3.6. Mineralogical Composition Analysis.** After 12, 24, 48, and 72 h of curing, the XRD analysis was performed to characterize the cement samples and examine the effect of curing time to adjust the hydrated cement's composition. The XRD results of Figure 11 show the changes in amorphous and portlandite content with curing time for the base cement and laponite-based samples. The amorphous phase was appearing at $2\theta$ values of 20.83, 26.61, 36.51, 39.43, 42.41, 45.79, 54.99, 59.95, and 68.29°, while the portlandite was appearing at 18.01, 28.67, 34.10, 47.12, and 50.81°.



https://doi.org/10.1021/acsomega.2c03491
ACS Omega 2022, 7, 31246−31259

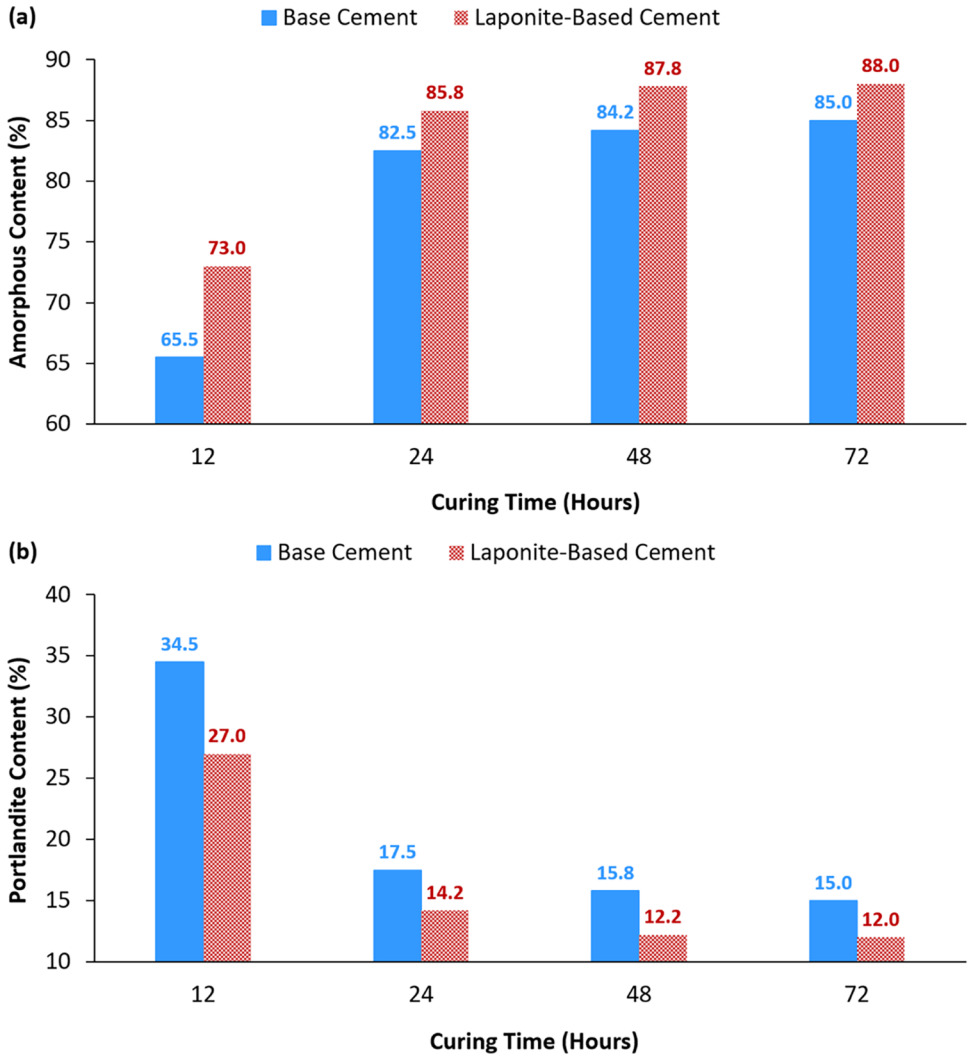


**Figure 11.** Content of (a) amorphous and (b) portlandite in the cement samples after 12, 24, 48, and 72 h of curing as characterized by XRD analysis.

As indicated in Figure 11a, the amorphous content for the laponite-based samples is higher than that for the base samples at all curing, while the portlandite content is higher in the base sample (Figure 11b).

The presence of lower portlandite content in the laponite-based samples is attributed to the high silica content in the laponite particles as reported earlier by Elkatatny.[14] The decrease in the portlandite content with time for both base and laponite-based samples is attributed to the progress of the pozzolanic reaction as explained by Massazza.[44] The progress of the pozzolanic reaction in base samples was because of the presence of silica flour, and that for the laponite-based samples was because of the presence of both silica flour and laponite particles. The higher amorphous content and lower portlandite content are the reason for the laponite-based samples to have higher strength (higher compressive and tensile strengths) and more elasticity (lower Young's modulus and higher Poisson's ratio).

## 4. CONCLUSIONS

The impact of laponite particles on the changes of the properties of class G oil well cement with curing time was investigated in this study. Cement samples with and without laponite were prepared, and the changes in their properties were evaluated at five different curing times of 6, 12, 24, 48, and 72 h. Based on the results, the following statements are drawn:

- The incorporation of laponite into well cement increased the compressive and tensile strengths of well cements compared to the strengths of a neat well cement, and the strength of both cement systems increased with the curing time.
- The addition of laponite decreased the permeability of the cement matrix compared with the neat cement at all curing times.
- The elasticity of the cement was improved by incorporating the laponite particles, as indicated by the decrease in Young's modulus and the increase in Poisson's ratio.
- Logarithmic relationships were established to represent the changes in the compressive and tensile strengths in addition to porosity, while the changes in the other properties of permeability, Poisson's ratio, Young's modulus, and density variation were represented accurately with power-law equations.



https://doi.org/10.1021/acsomega.2c03491
ACS Omega 2022, 7, 31246−31259

- The higher amorphous content and lower portlandite content are the reasons for the higher strength (higher compressive and tensile strengths) and higher elasticity (lower Young's modulus and higher Poisson's ratio) of laponite-based samples.

## AUTHOR INFORMATION


### Corresponding Author

**Salaheldin Elkatatny** − *Department of Petroleum Engineering, College of Petroleum Engineering and Geosciences, King Fahd University of Petroleum & Minerals, 31261 Dhahran, Saudi Arabia;* orcid.org/0000-0002-7209-3715; Email: elkatatny@kfupm.edu.sa

### Authors

**Abdulmalek Ahmed** − *Department of Petroleum Engineering, College of Petroleum Engineering and Geosciences, King Fahd University of Petroleum & Minerals, 31261 Dhahran, Saudi Arabia*

**Ahmed Abdulhamid Mahmoud** − *Department of Petroleum Engineering, College of Petroleum Engineering and Geosciences, King Fahd University of Petroleum & Minerals, 31261 Dhahran, Saudi Arabia*

Complete contact information is available at: https://pubs.acs.org/10.1021/acsomega.2c03491


### Notes

The authors declare no competing financial interest.

## ACKNOWLEDGMENTS

The authors thank King Fahd University of Petroleum & Minerals (KFUPM) for employing its resources in conducting this work.

## REFERENCES


(1) Nelson, E. B.; Guillot, D. *Well Cementing*, 2nd ed.; Schlumberger, 2006.

(2) Krakowiak, K. J.; Thomas, J.; Musso, S.; James, S.; Akono, A.; Ulm, F. Nano-chemo-mechanical signature of conventional oil-well cement systems: Effects of elevated temperature and curing time. *Cem. Concr. Res.* **2015**, *67*, 103−121.

(3) Ghadiri, M.; Hau, H.; Chrzanowski, W.; Agus, H.; Rohanizadeh, R. Laponite clay as a carrier for in situ delivery of tetracycline. *RSC Adv.* **2013**, *3*, 20193−20201.

(4) Negrete, J.; Letoffe; Putaux, J.; David, L.; Bourgeat-Lami, E. Aqueous Dispersions of Silane-Functionalized Laponite Clay Platelets. A First Step toward the Elaboration of Water-Based Polymer/Clay Nanocomposites. *Langmuir* **2004**, *20*, 1564−1571.

(5) Sun, K.; Kumar, R.; Falvey, D. E.; Raghavan, S. R. Photogelling colloidal dispersions based on light-activated assembly of nanoparticles. *J. Am. Chem. Soc.* **2009**, *131*, 7135−7141.

(6) Bienia, M.; Danglade, C.; Lecomte, A.; Brevier, J.; Pagnoux, C. Cylindrical Couette flow of Laponite dispersions. *Appl. Clay Sci.* **2018**, *162*, 83−89.

(7) Mohanty, R. P.; Joshi, Y. M. Chemical stability phase diagram of aqueous Laponite dispersions. *Appl. Clay Sci.* **2016**, *119*, 243−248.

(8) Thompson, D. W.; Butterworth, J. T. The nature of laponite and its aqueous dispersions. *J. Colloid Interface Sci.* **1992**, *151*, 236−243.

(9) Loginov, M.; Lebovka, N.; Vorobiev, E. Laponite assisted dispersion of carbon nanotubes in water. *J. Colloid Interface Sci.* **2012**, *365*, 127−136.

(10) Manilo, M. V.; Lebovka, N.; Barany, S. Characterization of the electric double layers of multi-walled carbon nanotubes, laponite and nanotube+laponite hybrids in aqueous suspensions. *Colloids Surf., A* **2014**, *462*, 211−216.

(11) Manilo, M. V.; Lebovka, N.; Barany, S. Combined effect of cetyltrimethylammonium bromide and laponite platelets on colloidal stability of carbon nanotubes in aqueous suspensions. *J. Mol. Liq.* **2017**, *235*, 104−110.

(12) Manilo, M. V.; Lebovka, N.; Barany, S. Stability of multi-walled carbon nanotube+laponite hybrid particles in aqueous suspensions. *Colloids Surf., A* **2015**, *481*, 199−206.

(13) Silva, J. M.; Barud, H. S.; Meneguin, A. B.; Constantino, V. R. L.; Ribeiro, S. J. L. Inorganic-organic bio-nanocomposite films based on Laponite and Cellulose Nanofibers (CNF). *Appl. Clay Sci.* **2019**, *168*, 428−435.

(14) Elkatatny, S. Development of a homogenous cement slurry using synthetic modified phyllosilicate while cementing HPHT wells. *Sustainability* **2019**, *11*, No. 1923.

(15) Liu, W.; Zhai, D.; Huan, Z.; Wu, C. J. Chang. Novel tricalcium silicate/magnesium phosphate composite bone cement having high compressive strength, in vitro bioactivity and cytocompatibility. *Acta Biomater.* **2015**, *21*, 217−227.

(16) Ghadiri, M.; Chrzanowski, W.; Rohanizadeh, R. Biomedical applications of cationic clay minerals. *RSC Adv.* **2015**, *5*, 29467−29481.

(17) Thiercelin, M. J.; Dargaud, B.; Baret, J. F.; Rodriguez, W. J. In *Cement Design Besed on Cement Mechanical Response*. Paper presented at the SPE Annual Technical Conference and Exhibition, San Antonio, Texas, SPE-38598-MS, Oct, 1997.

(18) Justnes, H.; Van Loo, D.; Reyniers, B.; Skalle, J.; Sveen, P.; Sellevold, E. J. Chemical shrinkage of oil well cement slurries. *Adv. Cem. Res.* **1995**, *7*, 85−90.

(19) Lyomov, S. K.; Backe, K. R.; Skalle, P.; Lile, O. B.; Justnes, H.; Sveen, J. In *Shrinkage of Oil Well Cement Slurries*, Paper presented at the Annual Technical Meeting, Calgary, Alberta, PETSOC-97-77, June, 1997.

(20) Parcevaux, P. A.; Sault, P. H. In *Cement Shrinkage and Elasticity: A New Approach for a Good*. Paper presented at the SPE Annual Technical Conference and Exhibition, Houston, Texas, SPE-13176-MS, Sept, 1984.

(21) Mahmoud, A. A.; Elkatatny, S. In *The Effect of Silica Content on the Changes in the Mechanical Properties of Class G Cement at High Temperature from Slurry to Set*. Paper presented at the 53rd U.S. Rock Mechanics/Geomechanics Symposium, New York City, New York, ARMA-2019-1816, June, 2019. https://onepetro.org/ARMAUSRMS/proceedings/ARMA19/All-ARMA19/ARMA-2019-1816/125024.

(22) Reinås, L.; Hodne, H.; Mirkamil, A. T. In *Hindered Strength Development in Oil Well Cement due to Low Curing Temperature*, Paper presented at the SPE Arctic and Extreme Environments Conference and Exhibition, Moscow, Russia, SPE-149687-MS, Oct, 2011.

(23) Parrott, L. J.; Geiker, M.; Gutteridge, W. A.; Killoh, D. Monitoring Portland cement hydration: comparison of methods. *Cem. Concr. Res.* **1990**, *20*, 919−926.

(24) Sant, G.; Dehadrai, M.; Bentz, D.; Lura, P.; Ferraris, C. F.; Bullard, J. W.; Weiss, J. Detecting the fluid-to-solid transition in cement pastes, comparing experimental and numerical techniques. *Concr. Int.* **2009**, *31*, 53−58.

(25) Sobolev, K.; Gutierrez, M. F. How nanotechnology can change the concrete world - Part one. *Am. Ceram. Soc. Bull.* **2005**, *84*, 14−17.

(26) Thomas, J. J.; Jennings, H. M.; Chen, J. J. Influence of nucleation seeding on the hydration mechanisms of tricalcium silicate and cement. *J. Phys. Chem. C* **2009**, *113*, 4327−4334.

(27) Jo, B.-W.; Kim, C.; Tae, G.; Park, J. Characteristics of cement mortar with nano-SiO2 particles. *Constr. Build. Mater.* **2007**, *21*, 1351−1355.

(28) Korpa, A.; Trettin, R.; Böttger, K. G.; Thieme, J.; Schmidt, C. Pozzolanic reactivity of nanoscale pyrogene oxides and their strength contribution in cement-based systems. *Adv. Cem. Res.* **2008**, *20*, 35−46.

(29) Land, G.; Stephan, D. The influence of nano-silica on the hydration of ordinary Portland cement. *J. Mater. Sci.* **2012**, *47*, 1011−1017.

(30) Amin, S. K.; Allam, M. E.; Garas, G. L.; Ezz, H. A. Study of the Chemical Effect of Marble and Granite Slurry on Green Mortar Compressive Strength. *Bull. Natl. Res. Cent.* **2020**, *44*, No. 19.
(31) Doneliene, J.; Eisinas, A.; Baltakys, K.; Bankauskaite, A. The Effect of Synthetic Hydrated Calcium Aluminate Additive on the Hydration Properties of OPC. *Adv. Mater. Sci. Eng.* **2016**, *2016*, No. 3605845.
(32) Brough, A. R.; Katz, A.; Sun, G. K.; Strubl, L. J.; Kirkpatrick, R. J.; Young, J. F. Adiabatically cured, alkali-activated cement based waste forms containing high levels of fly ash, formation of zeolites and Al-substituted C−S−H. *Cem. Concr. Res.* **2001**, *31*, 1437−1447.
(33) Hong, S. Y.; Glasser, F. P. Alkali sorption by C-S-H and C-A-SH gels: part II. Role of alumina. *Cem. Concr. Res.* **2002**, *32*, 1101−1111.
(34) Richardson, I. G. The nature of C−S−H in hardened cements. *Cem. Concr. Res.* **1999**, *29*, 1131−1147.
(35) Richardson, I. G.; Cabrera, J. G. The Nature of C−S−H in model slag-cements. *Cem. Concr. Compos.* **2000**, *22*, 259−266.
(36) Schneider, J.; Cincotto, M. A.; Panepucci, H. 29 Si and 27Al high resolution NMR characterization of calcium silicate hydrate phases in activated blast-furnace slag pastes. *Cem. Concr. Res.* **2001**, *31*, 993−1001.
(37) API. *Worldwide Cementing Practices*; API: Dallas, Texas, 1991.
(38) API. *API Recommended Practice 10B-2-Recommended Practice for Testing Well Cements*, 2nd ed.; American Petroleum Institute: Washington, 2013.
(39) ASTM C109/C109M. *Standard Test Method for Compressive Strength of Hydraulic Cement Mortars (Using 2-in. or [50-mm] Cube Specimens)*; ASTM International: West Conshohocken, PA, 2016. www.astm.org.
(40) ASTM D3967-16. *Standard Test Method for Splitting Tensile Strength of Intact Rock Core Specimens*; ASTM International: West Conshohocken, PA, 2016. www.astm.org.
(41) Mahmoud, A. A.; Elkatatny, S. Improved durability of Saudi Class G oil-well cement sheath in CO2 rich environments using olive waste. *Constr. Build. Mater.* **2020**, *262*, No. 120623.
(42) Murtaza, M.; Rahman, M.; Al Majed, A.; Tariq, Z.; Mahmoud, M. In *Scratch Test for Strength and Toughness of Oil Well Cement with Nanoclay as an Additive*. Paper Presented at the Abu Dhabi International Petroleum Exhibition & Conference, SPE-197681-MS, Nov 11−14, 2019.
(43) Fjaer, E.; Holt, R. M.; Horsrud, P.; Reean, A. M.; Risnes, R. *Petroleum Related Rock Mechanics*; 2nd ed.; Elsevier Science, 2007. ISBN-10: 0444502602.
(44) Massazza, F. Lea's Chemistry of Cement and Concrete. *Pozzolana and Pozzolanic Cements*, 4th ed.; Butterworth-Heinemann, 1998; Chapter 10, pp 471−635.



https://doi.org/10.1021/acsomega.2c03491
*ACS Omega* 2022, 7, 31246−31259